RSC Advances

This article can be cited before page numbers have been issued, to do this please use: T. Sun, L. Shu, J. Shen, C. Ruan, Z. Zhao and C. Jiang, *RSC Adv.*, 2016, DOI: 10.1039/C6RA05808F.

ROYAL SOCIETY OF CHEMISTRY

www.rsc.org/advances

View Article Online
DOI: 10.1039/C6RA05808F

Journal Name

ARTICLE

Photo and Redox-Responsive Vesicles Assembled From Bola-type Superamphiphiles

Received 00th January 20xx,
Accepted 00th January 20xx

DOI: 10.1039/x0xx00000x

www.rsc.org/

Tao Sun,[a] Lan Shu,[a] Jian Shen,[b] Chunhui Ruan,[a] Zhifeng Zhao[a] and Chen Jiang*[a]

Superamphiphiles are considered as a promising approach for fabricating stimuli-responsive materials. Sensitivity to more than one stimulus can improve the system's versatile performance. In this study, we proposed a facile dual-responsive vesicle constructed from Bola-type superamphiphiles. An *azo*benzene dimer linked by disulfide bond was synthesized. As the gust molecule, the *azo*benzene dimer can be included into the β-cyclodextrin's cavity from both ends to form a novel Bola-type superamphiphile, which can further assemble into vesicular structure in aqueous solution. The vesicles were characterized by transmission electron microscopy (TEM) and dynamic light scattering (DLS). The formation mechanism of the vesicular structure was suggested based on the NMR, Fourier transform infrared spectroscopy (FT-IR) and X-ray diffraction (XRD) results. The photo and redox responsiveness of the vesicles was studied. The vesicles were found capable to carry mitomycin C (MMC) and the drug-release can be greatly promoted upon UV irradiation or reductant.

Introduction

Narrowing the gap between the general concepts of molecular-recognition/self-assembly and their applications still remains a great challenge in current supramolecular chemistry.[1] In this regard, sophisticated stimuli-responsive materials have been well studied with the hope of usage in controllable release and molecular machine. Multiple means employing H-bonding, π-π stacking or metal-ligand coordination as the linkage, ambient condition factors like pH, redox, temperature and light as the "Turn-On" switches have been developed.[2~11] Among most stimuli-responsive materials, the triggers are always realized by adding heterogenous reagents to the initial systems,[12] which, however, could cause non-ignorable convective motion and mechanically injurious to fragile samples or living tissues.[13] *In situ* tailoring the aggregates in solution or intracellular in a noninvasive manner (for instance, heat,[14] ultrasound intensity,[15] electric pulses,[16] magnetism,[17] light[18] and endogenous glutathione (GSH) in tumor cells[19]) provides an attractive alternation without introducing new exogenous species. The combination of different noninvasive triggers into single responsive nanoarchitecture will provide multiple means to increase the responsive sensibility and realize the functions at aimed positions in a more controllable way.[20] For example, light as the trigger can realize a clean and precise spatio-temporal control, but meanwhile the low efficiency and poor penetrating ability prevents its further applications. Employing redox as the co-activator of the system can enhance the responding efficacy and combine the advantages of both triggers.

Superamphiphiles,[1~3] with hydrophilic and hydrophobic moieties linked *via* non-covalent bonds, are regarded as convenient and promising "building blocks" in preparing versatile stimuli-responsive materials.[2] To our knowledge, however, no reports on photo and redox responsive superamphiphlies were found. The dual-responsive approach employing exogenous (light) and endogenous (redox) triggers both in a noninvasive way should be of pronounced advantage in the pharmaceutical and biomedical sciences.

Sugar-based materials have been extensively explored as a means to increase bio-oriented systems' biocompatibility and biodegradation.[21] Cyclodextrins (CDs), a class of biocompatible truncated-cone polysaccharides mainly composed of 6~8 *D*-glucosemonomers (correspondingly named as α, β and γ-CD respectively) with hydrophilic exterior and hydrophobic interior, are known able to encapsulate many model substrates to form host-guest complexes.[22] Vesicles enclose membranes consisting of a bilayer or multilayer of amphiphiles and a volume of water in the core, can carry hydrophilic and hydrophobic molecules simultaneously and attract increasing attention with the hope of promising applications in drug/gene delivery,[23] nanoreactors[24] and artificial cell membranes.[25]

Herein, we report a photo- and redox-responsive superamphiphile constructed from an inclusion complexation of β-CD and disulfide-linked *azo*benzene dimer **1**. The *azo*benzene dimer **1** was designed, synthesized and fully characterized. The superamphiphiles can self-assemble into vesicles in aqueous solution. TEM and DLS were employed to characterize the vesicles' size and micromorphology. The formation mechanism was revealed based on the results of ^{1}H NMR, NMR-NOESY, FT-IR, XPRD and UV-vis spectrometer. The vesicles tend to be disrupted upon the introduction of dithiothreitol (DTT) and irradiation of UV light. The vesicles were found able to carry the model drug and the drug release can be promoted by UV light and reductant *in vitro*. This novel photo and redox responsive vesicles based on superamphiphiles are promising materials in meeting the

[a] Key Laboratory of Smart Drug Delivery (Ministry of Education), State Key Laboratory of Medical Neurobiology, Department of Pharmaceutics, School of Pharmacy, Fudan University, Shanghai 201203, PR China.
[b] School of Chemistry and Chemical Engineering, Weifang University, Weifang 261061, PR China.
† jiangchen@shmu.edu.cn.
Electronic Supplementary Information (ESI) available: detailed synthesis and mechanism study. See DOI: 10.1039/x0xx00000x

requirements for functional, regular, well-defined, and stimuli-responsive nanoarchitectures, which could be further used in the fields of drug delivery, molecular machine, and nanoreactor.

Experimental section

Materials

β-CD was a gift from Zhiyuan Biotechnology Co. Ltd. (Binzhou, China), recrystallized twice in water, and dried under vacuum at 50 °C for 12 h before using. *p*-Hydroxyazobenzene, 1,4-dibromobutane thiourea, DTT and GSH were purchased from Aladdin (Shanghai, China). 2, 2'-Dithiobispyridine was from TCI Europe (Eschborn, Germany). Agents including DMSO-δ6, CD_3OD and $CDCl_3$ for nuclear magnetic resonance (NMR) spectroscopy were from J&K Scientific Ltd. (Beijing, China). HCl, KOH and all the solvents mentioned here were from Sinopharm Chemical Reagent (Shanghai, China). Silica gel for flash column chromatography (SilicaFlash F60, 230~400 mesh) was from Haiyang Chemical Co., Ltd. (Qingdao, China). N_2 and Ar were from Chenggong Gas (Shanghai, China). MMC was from Knowshine Pharmachemicals Inc. (Shanghai, China). PBS (pH = 7.40) buffer was prepared by adding NaCl (8 g), $Na_2HPO_4{\cdot}12H_2O$ (2.9 g), KCl (0.2 g), and KH_2PO_4 (0.2 g) into 1000 mL distilled water, and then the mixture was sonicated for 20 min at 300 K. All chemicals were used as received unless indicated otherwise.

Analytical Measurements and Methods.

Proton-1 NMR (^{1}H NMR) spectra were recorded on a Varian Oxford NMR spectrometer (Palo Alto, California, USA) operating at 400 MHz/25 °C, while carbon-13 NMR (^{13}C NMR) and NMR ROESY spectra were recorded on a Bruker NMR Ascend 600 spectrometer (Billerica, Massachusetts, USA) operating at 600 MHz/25 °C. Fourier transform infrared spectroscopy (FTIR) spectra were obtained using ATR geometry on a Spectrum 65 infrared spectrophotometer (Perkin-Elmer, Waltham, Massachusetts, USA) at 25 °C. Mass spectrometry (MS-ESI) data were obtained from Agilent LCMSD (Santa Clara, California, USA). All TEM observations were carried on a JEM-100CX electron microscope from JEOL Ltd. (Tokyo, Japan). *Cryo*-TEM was recorded with a JEOL JEM-1400 TEM (120 kV) at −174 °C cooled by liquid nitrogen. DLS measurements were carried out with a Wyatt QELS Technology DAWN HELEOS instrument (Santa Barbara, USA) poised at constant room temperature (25 °C) by using a 12-angle replaced detector in a scintillation vial and a 50 mW solid-state laser (λ = 658.0 nm). All solutions for DLS were filtered through a 0.45 μm filter before measurement. MM2 energy minimize and molecular size calculation was undertaken on ChemBio 3D Ultra (14.0 version, Cambridge Software, Massachusetts, USA). Drug-release was monitored by analytical HPLC, with a Dionex system equipped with gradient flow control pump (Merck HITACHI pump L-7100, Dartford, UK), autosampler (Merck HITACHI L-7200, Dartford, UK), Merck HITACHI Interface L-7000 (Dartford, UK), solvent degasser (Merck L-7612, Dartford, UK), autosampler, diode array detector (DAD, Merck HITACHI L-7455, Dartford, UK), fluorescence detector (Merck HITACHI FL L-7485, Dartford, UK) and column oven (Merck L-7360, Dartford, UK). All the parameters of HPLC were controlled by LC solutions software Ezchrom Elite (SIM GmbH, Oberhausen, Germany). A LiChroCART® 250-4 column (100 RP-18 (5 μm), Merck KGaA, Darmstadt, Germany) was employed for the HPLC analysis of MMC. A UV detector with wavelength from 200 to 600 nm was used and the absorbance was recorded at 365 nm. An isocratic mobile phase of 15% acetonitrile in 10 mM phosphate buffer (pH 6.5) in 18 min at a 1 mL/min flow rate was used. The R_t of the analyte (MMC) and the internal standard (riboflavin) are 7.8 and 6.7 min, respectively.

Synthesis of the compounds

Compound **2**: Compounds **2** and **3** were synthesized in a similar way as reported.[26] Commercial available *p*-hydroxyazobenzene (1.98 g, 10 mmol, 1 eq), 1,4-dibromobutane (7.1 mL, 60 mmol, 6 eq) and KOH (1.12 g, 20 mmol, 2 eq) in pure EtOH (150 mL) was refluxed under an atmosphere of N_2 for 12 h. After cooling down to r.t., EtOH was removed under reduced pressure. Dichloromethane (DCM, 100 mL) was added to the resulting residue and the solid was filtered off. DCM was removed *in vacuo* and the crude product was purified by a flash column chromatography (SiO_2, ethyl acetate/petroleum ether (PE), from 1/10 to 1/5 v/v). **2** (1.50 g, 45%) was obtained as a dark brown powder.

R_f = 0.9 (ethyl acetate/PE, 1/8 v/v); ^{1}H NMR (400 MHz, $CDCl_3$, δ, ppm): 7.92 (d, J = 8.8 Hz, 2H), 7.88 (d, J = 7.6 Hz, 2H), 7.51 (t, J = 7.6 Hz, 2H), 7.45 (dd, J_1= 6.0 Hz, J_2= 7.6 Hz, 1H), 7.01 (d, J = 8.8 Hz, 2H), 4.09 (t, J = 6.4 Hz, 2H), 3.51 (t, J = 6.4 Hz, 2H), 2.09 (m, 2H), 2.00 (m, 2H); ^{13}C NMR (600 MHz, $CDCl_3$, δ, ppm): 160.8, 152.1, 146.3, 129.8 (2C), 128.4 (2C), 124.2 (2C), 121.9 (2C), 66.6, 32.7, 28.8, 27.2;MS-ESI Calc. for $C_{16}H_{18}BrN_2O$ $[M+H]^+$ 333.1 (100%) and 335.1 (97%), Found, 333.0 (100%) and 335.0 (97%); IR ($\nu_{cm\text{-}1}$): 2880.0 (m, $\nu_{CH2\text{-}O\text{-}Ar}$), 1605.2 (vs, $\nu_{N=N}$), 1258.2 (s, $w_{CH2\text{-}S}$), 776.4 (m, ν_{CH}), 689.7 (s, $\nu_{C\text{-}Br}$).

Compound **3**: A solution of 2 (0.19 g, 0.57 mmol, 1 eq) and thiourea (0.22 g, 2.89 mmol) in EtOH (10 mL) was heated under reflux for 12 h. After cooling down to r.t., a solution of KOH (0.19 g, 3.47 mmol) in H_2O (10 mL) was then added into the above solution, refluxed for another 3 h and cooled down to r.t.. The mixture was acidified by HCl (1N) to pH = 1 and extracted by Et_2O (30 mL×3). Organics were combined and washed with brine, dried over Na_2SO_4. The solvent was removed *in vacuo* and the crude product was purified by a flash column chromatography (SiO_2, ethyl acetate/PE, 1/5 v/v). **3** (0.12 g, 75%) was obtained as a brown oil.

R_f = 0.8 (ethyl acetate/PE, 1/5 v/v); ^{1}H NMR (400 MHz, $CDCl_3$, δ, ppm): 7.92 (d, J = 8.8 Hz, 2H), 7.88 (d, J = 7.6 Hz, 2H), 7.51 (t, J = 7.6 Hz, 2H), 7.45 (dd, J_1= 6.0 Hz, J_2= 7.6 Hz, 1H), 7.00 (d, J = 8.8 Hz, 2H), 4.07 (t, J = 6.4 Hz, 2H), 2.64 (dd, J_1 = 6.8 Hz, J_2 = 7.2 Hz, 2H), 1.95 (m, 2H), 1.85 (m, 2H), 1.58 (m, 1H); ^{13}C NMR (600 MHz, $CDCl_3$, δ, ppm): 161.0, 151.8, 146.1, 129.8, 128.4 (2C), 124.4 (2C), 121.9 (2C), 114.1 (2C), 67.1, 29.9, 27.3, 23.8; MS-ESI Calc. for $C_{16}H_{19}N_2OS$ $[M+H]^+$ 287.1, Found, 287.0; IR ($\nu_{cm\text{-}1}$): 2934.3 (vs, $\nu_{CH2\ linking\ SH}$), 2872.3 (m, $\nu_{CH2\text{-}O\text{-}Ar}$), 1600.5 (vs, $\nu_{N=N}$), 1253.5 (vs, $w_{CH2\text{-}S}$), 767.1 (m, ν_{CH}), 686.6 (m, $\nu_{C\text{-}SH}$).

Compound **4**: To a stirred solution of 2, 2'-dithiobispyridine (440 mg, 2 mmol, 4 eq) in AcOH/EtOH (1/20 v/v, 10 mL, degassed by N_2 for 3 min), **3** (143 mg, 0.5 mmol, 1 eq) in AcOH/EtOH (1/20 v/v, 5 mL, degassed with N_2 for 3 min) was injected dropwise over 20 min under an atmosphere of N_2. The mixture was allowed to react at r.t. for 12 h. The solvents were then evaporated to dryness *in vacuo*. The resulting residue was subjected to a flash column chromatography (SiO_2, ethyl acetate/PE, from 1/9 to 1/4 v/v) to afford **4** (73 mg, 37%) as an orange powder.

R_f = 0.3 (ethyl acetate/PE, 1/8 v/v); ^{1}H NMR (400 MHz, $CDCl_3$, δ, ppm): 8.48 (d, J = 4.4 Hz,1H), 7.90 (d, J = 8.8 Hz, 2H), 7.88 (d, J = 9.2 Hz, 2H), 7.74 (d, J = 8.0 Hz, 1H), 7.66 (t, J = 8.0 Hz, 1H), 7.50 (t, J = 7.6 Hz, 2H), 7.45 (dd, J_1= 7.2 Hz, J_2= 7.6 Hz, 1H), 7.10 (t, J = 6.0 Hz, 1H), 6.97 (d, J = 8.4 Hz, 2H), 4.04 (t, J = 6.4 Hz, 2H), 2.90 (t, J = 6.4 Hz, 2H), 1.94 (m,

4H); ^{13}C NMR (600 MHz, $CDCl_3$, δ, ppm): 160.8, 159.6, 152.1, 148.6, 146.4, 136.8, 129.7, 128.4 (2C), 124.1 (2C), 121.9 (2C), 120.1, 119.4, 114.1 (2C), 67.0, 37.9, 27.3, 24.9; MS-ESI Calc. for $C_{21}H_{22}N_3OS_2$ $[M+H]^+$ 396.1, Found, 396.0; IR (ν_{cm-1}): 3042.7 (m, $\nu_{CH\ of\ pyridine}$), 2867.6 (m, $\nu_{CH2-O-Ar}$), 1600.5 (vs, $\nu_{N=N}$), 1248.9 (vs, w_{CH2-S}), 1041.3 (m, $w_{pyridine\ ring}$), 826.0 (s, $\gamma_{CH\ of\ pyridine}$), 771.8 (m, ν_{CH}), 722.2 (m, ν_{C-S}).

Compound **1**: To a stirred solution of **4** (80 mg, 0.2 mmol, 1 eq) in AcOH/EtOH (1/20 v/v, 10 mL, degassed by N_2 for 3 min), **3** (143 mg, 0.5 mmol, 2.5 eq) in AcOH/EtOH (1/20 v/v, 5 mL, degassed with N_2 for 3 min) was injected dropwise over 20 min under an atmosphere of N_2. The mixture was allowed to react at r.t. for 12 h. The solvents were then removed *in vacuo*. The resulting residue was subjected to a flash column chromatography (SiO_2, ethyl acetate/PE, 1/8 v/v) to afford **1** (38 mg, 33%) as an orange powder.

R_f = 0.7 (ethyl acetate/PE, 1/8 v/v); ^1H NMR (400 MHz, $CDCl_3$, δ, ppm): 7.91 (d, J = 8.8 Hz, 4H), 7.87 (d, J = 7.2 Hz, 4H), 7.50 (t, J = 7.2 Hz, 4H), 7.44 (dd, J_1= 6.8 Hz, J_2= 7.2 Hz, 2H), 7.00 (d, J = 8.8 Hz, 4H), 4.07 (t, J = 6.4 Hz, 4H), 2.80 (t, J = 6.4 Hz, 4H), 1.93 (m, 4H), 1.94 (m, 8H); ^{13}C NMR (600 MHz, $CDCl_3$, δ, ppm): 160.9 (2C), 152.1 (2C), 146.3 (2C), 129.7 (2C), 128.4 (4C), 124.2 (4C), 121.9 (4C), 114.1 (4C), 67.1 (2C), 38.0 (2C), 29.1 (2C), 27.3 (2C), 25.1 (2C); MS-ESI Calc. for $C_{32}H_{35}N_4O_2S_2$ $[M+H]^+$ 571.2, Found, 571.2; HR-MS-TOF Calc. for $C_{32}H_{35}N_4O_2S_2$ $[M+H]^+$ 571.2201, Found, 571.2214; IR (ν_{cm-1}): 2861.0 (m, $\nu_{CH2-O-Ar}$), 1600.8 (vs, $\nu_{N=N}$), 1258.2 (s, w_{CH2-S}), 1136.1 (m, $\nu_{CH2-O-Ar}$), 839 (m, γ_{CH}), 763.6 (m, ν_{CH}), 482.4 (w, ν_{S-S}).

Preparation of the vesicles.

The β-CD/**1** vesicles' preparation procedure was followed as previously reported.[27] Typically, the vesicles were prepared by slowly adding drips of **1**'s ethanol solution into the β-CD aqueous solution over 5 min at 10 °C. Bluish opalescence appeared immediately, indicating the formation of assembled particles. The mixture was treated by vortex and then sonicated for 30 min, and ethanol was removed under vacuum or dialysis at room temperature.

Preparation of the TEM and *cryo*-TEM samples

All TEM samples were freshly prepared *via* the phosphotungstic acid staining technique: the copper mesh was dripped into the sample solution and air-dried, then a drop of phosphotungstic acid aqueous solution (0.5%) was dripped onto the mesh and baked under the infrared lamp for 20 min. *Cryo*-TEM samples were prepared in a controlled environment vitrification system (CEVS) at 25 ◦C. A micropipette was employed to load 5 µL solution onto a TEM copper grid, which was then blotted with filter paper, resulting in the formation of thin films suspended on the mesh holes. After 5 s, the samples were quickly plunged into a reservoir of liquid ethane (cooled and kept by liquid nitrogen) at −165 ◦C. The vitrified samples were then stored in liquid nitrogen until they were completely transferred to a cryogenic sample holder (Gatan 626) and examined with a JEOL JEM-1400 TEM (120 kV) at −174 ◦C cooled by liquid nitrogen. The phase contrast was enhanced by under-focus. The images were recorded on a Gatan multiscan CCD and processed with Digital Micrograph.

Preparation of the β-CD/1 inclusion complex and the physical mixture.

The sample of β-CD/**1** inclusion complex for FT-IR and XRD characterizations were isolated by freeze-drying the vesicular β-CD/**1** aqueous solution samples. The physical mixture was obtained by simply mixing compound **1** and β-CD together with the same molar ratio as the inclusion. The mixture should be freshly prepared to avoid the possible complexion activity between the host and guest molecules during the placed period. It should be noted that for FTIR spectra, the physical mixture sample β-CD and compound **1** should be grinded with dry KBr separately, then mixed together quickly and tableted into a single cake, in order to weaken the possible inclusion phenomenon between them during the grinding procedure.[28]

Preparation of samples for Job's plots and complex constant.

The complex stoichiometry of β-CD with compound **1** in water was determined by Job's continuous variation method using a UV-vis spectrometer. A set of working solutions were obtained by mixing Vg mL of the stock **1** solution (10^{-4} mol/L) with (V_t-V_g) mL of the stock β-CD solution (10^{-4} mol/L), where V_t is a fixed total volume and V_g is a variable value (from 0 to 10 mL, $0 \le V_g \le V_t$). To obtain the complex constant, the concentration of **1** (2×10^{-5} mol/L) was kept constant with the concentration of β-CD ranging from 4×10^{-4} mol/L to 3.6×10^{-3} mol/L.

Photo-responsive property

UV irradiation (365 nm, 60 mW·cm^{-2}) and irradiation by visible light (λ = 434 nm, 20 mW·cm^{-2}) were carried out with a ZF-20D UV analyzer (Chengxian Instrument Co., Ltd. (Shanghai, China). It should be noted that the samples for DLS, TEM, NMR or UV-vis measurement should be well sealed in order to avoid possible solvent evaporation. The treated samples should be vortexed again for 3 min before measured.

Redox-responsive property

Before DLS and TEM detection, excess DTT was added to the vesicular sample and vortexed vigorously for 15 min at 300 K. Notably, no filtrate screening procedure by 0.45 µm filter was carried out before DLS measurement unless indicated.

Drug loading and release

MMC solution (218 µL) dissolved in methanol with a concentration of 55 mg/mL was dispersed in 6 mL vesicular solution (5×10^{-4} mol/L) at room temperature under vigorous vortex. Methanol was removed employing a rotary evaporator at 300 K. After vortex and sonication for 5 min respectively, the dispersion was treated on table concentrator at 4 °C for 5 min. The solid was removed by centrifugation (2 000 *g*), while the supernatant was distributed equally into 3 dialysis bags (3 × 1 mL, CE MWCO 500) for the drug-release test. The vesicular solution loading with MMC was dialyzed against pure water (25 mL). At the indicated incubation times, 20 µL solution was transferred into a closed tube containing riboflavin solution (80 µL, 100 µg/mL). The tube was vortexed with continuous mixing over 30 s, and 20 µL solution was submitted for HPLC analysis. The integral of the peaks of MMC and riboflavin was recorded. The pyrene-loading attempt was undertaken using a similar protocol.

To determine the drug loading rate and entrapment efficiency, 40 µL of the MMC-loading vesicular solution before dialysis treatment was transferred into a closed tube containing riboflavin aqueous solution (60 µL, 100 µg/mL). The tube was vortexed with continuous mixing over 30 s, and 20 µL solution was submitted for HPLC analysis.

The drug-release promoted by UV was realized by irradiation of the sample under UV light (365 nm, 60 mW·cm^{-2}) for 30 min. The drug-release promoted by reductant was realized by direct addition of excess DTT solid into the dialysis bags.

Results and discussion

Design, synthesis and characterization of 1

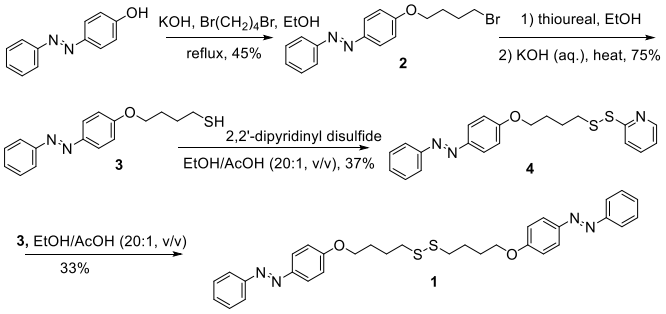

With the aim of designing photo and redox-responsive vesicles, a modularly approach were employed to construct the building block. The photo-responsiveness of *azo*benzene/β-CD complex and redox-responsiveness of disulfide bond were used in the molecular design. Then, a retrosynthesis was carried on and a classic method[11] was adopted to form the key disulfide bond *via* an intermediate of 2-mercaptopyridine derivate **4**. All compounds were characterized in detail (Figure S1 to S17, including ^{1}H NMR, ^{13}C NMR, MS, HR-MS-TOF and FT-IR spectra).

Morphologies and sizes of the vesicles

β-CD aqueous solution exhibited a typical true solution, whereas **1** aqueous dispersion can generate obvious cloudy suspension and some precipitation will appear if left to stand still for 2 h. The vesicular solution exhibited a slightly milky opalescence and totally differed from the samples with single compositions (Figure S18), indicating the formation of assembled particles.[27, 29] Typical Tyndall phenomenon of the β-CD/**1** vesicular solution was observed when a laser pointer was used to light the sample (Figure S18).

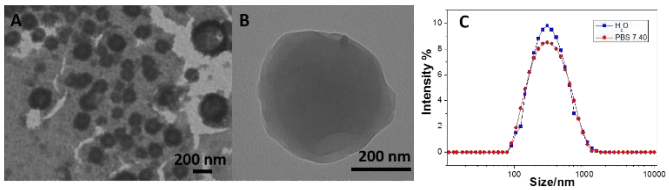

Figure 1. TEM micromorphology images (A: in water, B: in PBS) and DLS result (C) of β-CD/**1** vesicular sample. Phosphotungstic acid was used as the negative staining agent.

To demonstrate the microstructures of the self-aggregation, TEM[29, 30] and DLS[16, 18, 31] was used to study the morphologies of β-CD/**1** sample in pure water and PBS.

The TEM results in Figure 1 (A) and (B) show clear empty shells with obvious contrast between the center and the verge, which is the typical characteristic of vesicular aggregates based on the classical literatures.[2, 4, 32,33] and our experience.[34] To further verify the onion-like structure, *cryo*-TEM was undertaken as shown in Figure S19. The overall layer thicknesses of these vesicles was measured to be around 20 nm from TEM images. The layer thickness values are close to the long-axis dimensions of 2β-CD@**1** supramolecular system (Figure S20), suggesting a single-layered molecular packing model. The spherical morphology suggests a favourable rigid property to withstand the electron impact from TEM observation. The diameters of the obtained spheres are ranged from 100 to 800 nm. No vesicles were detected in the suspension of sole β-CD (irregular particles, Figure S21) or **1** (crystalline particles, Figure S22), demonstrating the importance of the combination with the supramolecular host and guest in forming the vesicular aggregates. To be more exact, DLS measurement was employed to further measure the particle size distributions (Figure 1 (C)), which gave an average diameter as 282.2 nm in pure water and 312.5 nm in PBS, which is slightly larger than the diameters obtained by TEM. It is understandable that TEM measures the solid spheres, whereas DLS measures the hydrodynamic diameters.[35] The polydispersion of the size distribution in DLS results is also in agreement with the TEM morphology. There are few differences in the size and morphology change observed by DLS and TEM one week after the preparation of the vesicular solution. .

Driving force of the vesicular formation

The knowledge on the know-how mechanism of the microstructure's formation is regarded crucial in guiding the initial structure design and tailoring the corresponding properties.[36] Multiple means, including XRD, FTIR, ^{1}H NMR, NMR-NOESY and UV-vis, were employed to investigate the mechanism of the vesicles' formation.

XRD analysis

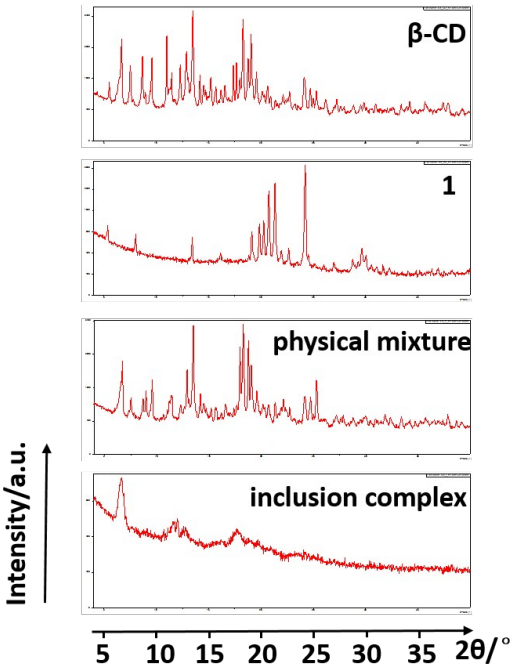

Figure 2. The XRD spectra of β-CD, **1**, their physical mixture, and inclusion complex at 300 K.

XRD[37] was applied in analyzing the species in the supramolecular complex (Figure 2). Freeze-dried β-CD/**1** complex, which can maintain the *in situ* dimensional molecular position,[38] was prepared.

View Article Online
DOI: 10.1039/C6RA05808F

In the β-CD/**1** physical mixture spectra, the peaks at 9.6◦, 12.7◦, 13.3◦ and 18.2◦ were found, evidencing β-CD molecules with a cage-type crystalline structure,[39] and in herringbone-type and brick-type.[40] The physical mixture is obviously an overlying of β-CD and **1**, whereas the β-CD/**1** complex is more like in an amorphous state, suggesting the formation of a new specie.

FTIR analysis

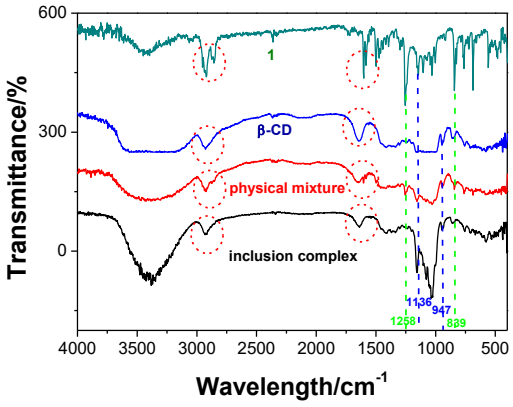

Figure 3. FT-IR spectra comparison of β-CD, **1**, their physical mixture, and inclusion complex in KBr capsules at 300 K.

FT-IR is widely employed in investigating the interactions among molecular in supramolecular science.[41] The solid supramolecular inclusion complex was obtained from the vesicular solution by freeze-drying, which is supposed able to maintain the *in-situ* interactions. The FT-IR spectral comparison of **1**, β-CD, their physical mixture, and the inclusion complex was undertaken as shown in Figure 3. Both the characteristic peaks of **1** (the blue dotted lines, 1136 cm^{-1}: $\nu_{CH2\text{-}O\text{-}Ar}$) and β-CD (947 cm^{-1}: $\nu_{C\text{-}O}$) can be found in the spectra of the physical mixture and inclusion complex, suggesting the composition of **1** and β-CD in them. The spectrum of the inclusion complex shows obvious differences from the physical mixture's: (1) based on the red-circled area, it is obvious to recognize that the physical mixture spectrum is the simple overlap of **1** and β-CD ones. Both **1** and β-CD are thus supposed to exist in an independent status; (2) in the inclusion complex, the peaks of $w_{CH2\text{-}S}$ (1268 cm^{-1}) and γ_{CH} (839 cm^{-1}) in **1**'s spectrum shifted or disappeared, evidencing the formation of a new specie; (3) the stretching vibration peaks of the hydroxyl group appearing near the wavelength of 3350 cm^{-1} are obviously different both in shape and in intensity, indicating the newly formed hydrogen bonds in the inclusion complex.[42]

^{1}H NMR characterizations

Table 1. ^{1}H NMR: comparison of the chemical shifts of single β-CD and β-CD/**1**[a]

Entry	H1	H2	H3	H4	H5	H6
δ(β-CD)	5.028	3.606	3.926	3.543	3.837	3.814
δ(β-CD/**1**)	5.020	3.598	3.914	3.537	3.825	3.798
$\Delta\delta^b$	0.008	0.008	0.012	0.006	0.012	0.016

[a]DHO peak (δ = 4.790) is as the interior label.

[b]$\Delta\delta = \delta$(β-CD) - δ(β-CD/**1**).

^{1}H NMR, as one of the most powerful and versatile methods in studying the supramolecular interactions in aqueous solutions,[43] was employed to investigate the mechanism. The comparison of ^{1}H NMR results of β-CD and β-CD/**1** samples was shown in Table 1 and Figure S23. It is known that H2 and H4 protons are located outside of the cyclodextrin cavity, while H3 and H5 protons are located inside the cavity[43]. From the table, it is easy to find out that both H3 and H5 protons exhibit slightly larger chemical shifts than H1, H2 and H4 proton, which means that **1** molecule is included into the cyclodextrin cavity. Meanwhile, H6 proton existing on the primary face also shows obvious chemical shift, indicating the guest molecule enter the cavity from the primary side[43]. During the supramolecular inclusion procedure, there is no change of covalent bonds and the chemical shifts are more ascribed to the micro environmental differences, mainly including: (1) the substitution of H_2O molecules in high energy state in the cavity by the *azo* moiety of compound **1**; (2) the hydrodynamic radius change after the complexation; (3) the destruction and formation of hydrogen bonds. The chemical shifts are thus not as pronounced as the ones resulted from the covalent bonds.

NMR NOESY

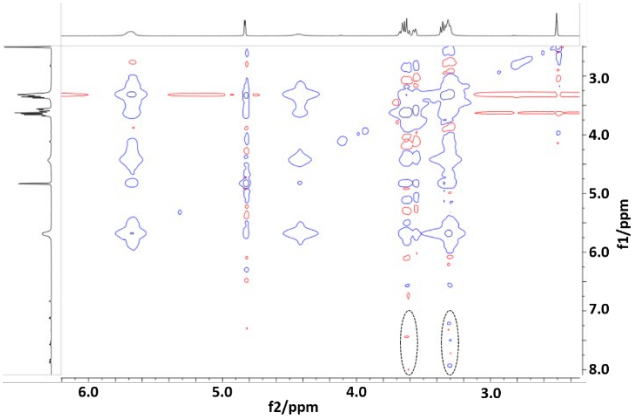

Figure 4. 2D NMR ROESY (600 MHz) spectrum of β-CD/**1** in DMSO-δ6 at T = 300 K.

2D NMR nuclear overhauser enhancement spectroscopy (2D NMR ROESY) is a reliable and versatile tool in detecting the interactions between pairs of nuclei that are closer than 5 Å, even if not covalently bound.[44] The solubility of β-CD/**1** in D_2O is too low to show the NMR peaks, DMSO-δ6 was used instead. Clear cross correlation between the signals of the inner CD protons (3.3 and 3.6 ppm) and the phenyl-protons of **1** (from 7 to 8 ppm) were found (Figure 4), demonstrating the entrance of **1** into β-CD cavity. Meanwhile, no interactions were found between **1** and H1 (locating outside the CD cavity), further evidencing the supposed inclusion model.

UV-vis spectra

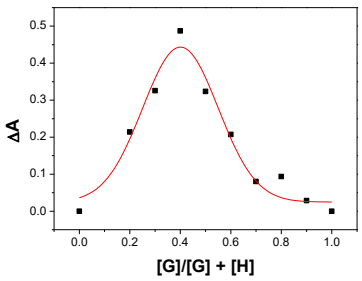

Figure 5. Job's plots by UV–vis for the binding of β-CD with compound **1** in water at room temperature.

The complex stoichiometry of β-CD with **1** in water was measured by the continuous variation method (Job's method) using a UV-vis spectrophotometer.[45] The Job's plots for the binding of β-CD with **1** in water showed a maximum value at a molar fraction of 0.4 (Figure S24, Figure 5), suggesting that **1**/β-CD complex stays in a 1:2 stoichiometry mode.[46] The result is also in accordance with previous study.[47] The stoichiometry and the inclusion constants were further calculated by UV double-reciprocal method based on the Benesi-Hildebrand equation:[48]

$$1/\Delta A = 1/\alpha + 1/\alpha Kap[\beta\text{-CD}]^n$$

Where ΔA is the change of UV absorbance of **1** in presence of β-CD, α is a constant, [β-CD] is the initial concentration of β-CD. *Kap* is the constant for the formation of n:1 (H:G) inclusion complex, which could be calculated from a plot of 1/ΔA versus 1/[β-CD]^n (Figure S25). The inclusion constants of 2:1 (H:G) were calculated as 3.69 × 10^6 L^2/mol^2.

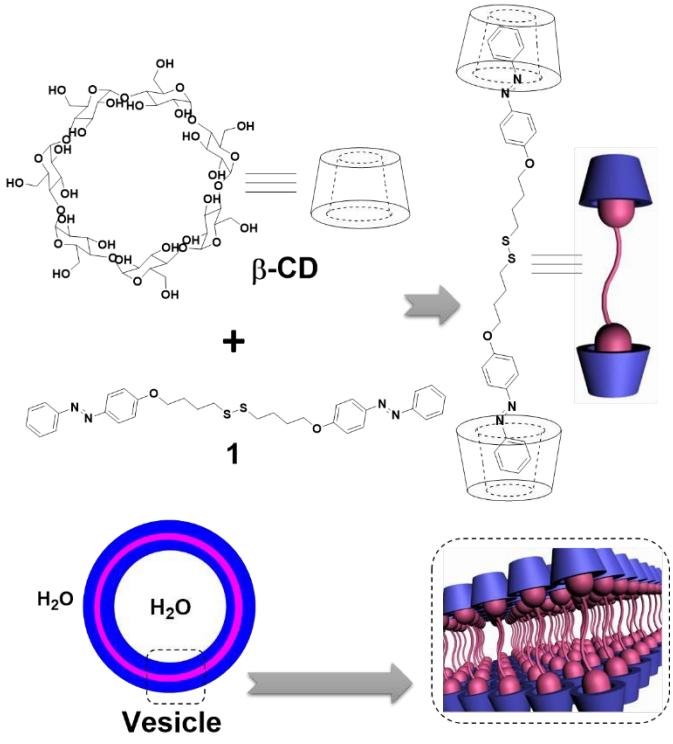

Scheme 1. Illustration of the formation mechanism for the vesicle and "Bola-type" superamphiphiles

β-CD, with a hydrophobic inner dimensional cavity and hydrophilic rims, have the capability to encapsulate or trap hydrophobic substrate to form a supramolecular inclusion complex in aqueous solution.[49] The host-guest binding is normally based on the non-covalent interactions, and thus reversible. Based on the analysis of the molecular structures (Figure S20) and the above experimental results, compound **1** as the guest molecule could be recognized and caged by the host molecule *via* hydrogen bonds, hydrophobic and *van der Waals* interactions.[50] The both-ended benzene rings of **1** molecule enter the β-CD cavity through the primary face, while the –N=N– moiety remains outside the cavity, participating with the hydroxyl groups in the rims *via* hydrogen bonds. In this way, the constructed "Bola" superamphiphiles can be homogeneously dispersed in water and self-assemble into bilayer vesicles. The "sandwich"-like bilayer membrane is illustrated in Scheme 1: the hydrophilic β-CD heads interact with surrounding water and hydrophobic linkers minimize their exposure to water by aggregating together. The vesicles' formation mechanism can be concluded into two levels of supramolecular assembly: construction of superamphiphiles based on host-guest recognition and organization of the superamphiphiles into vesicular structure. Different topology structures will lead different properties and corresponding functions. Since there are very few reports on "Bola-type" superamphiphile, enriching the topology structure of superamphiphile is regarded valuable.

Photo-reversible

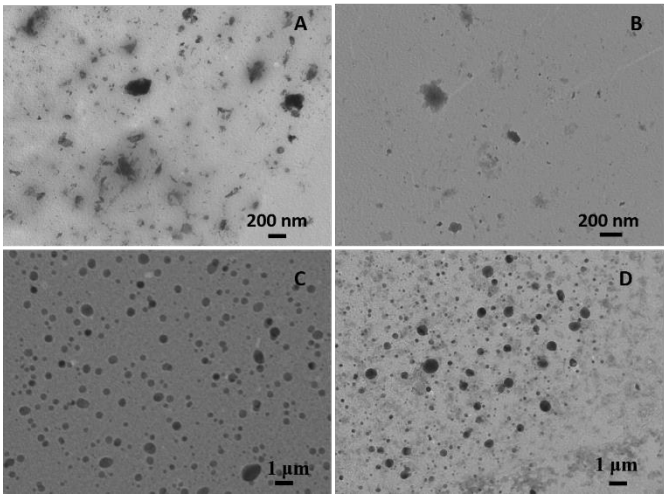

Figure 6. TEM micromorphology images of β-CD**/1** samples (A) UV-irradiated in water; (B) UV-irradiated in PBS; (C) visible light-irradiated in water; (D) visible light-irradiated in PBS, where the irregular particles could be ascribed to the dried inorganic salts in PBS. Phosphotungstic acid was employed as the negative staining agent.

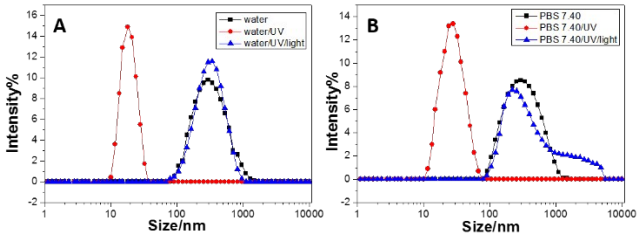

Figure 7. DLS size distributions of β-CD/**1** vesicles, UV-irradiated sample (30 min) and visible-light-irradiated sample (5 h) in water (A) and PBS 7.40 buffer (B).

Table 2. DLS results of the vesicles in the aqueous solution at 300 K upon UV (0.5 h) and visible light (5 h) irradiation.

Media	Initial	Upon UV irradiation (0.5 h)	Upon visible light irradiation (5 h)
pure water[a]	282.2	30.8	297.6
PBS 7.40[a]	312.5	48.7	343.4

[a]The unit is nm.

Light, as a non-invasive regulating approach, has its special advantages over chemical triggers. For instance, it takes several minutes for chemical triggers to reach the target, while it takes less than one second for light[13]. Furthermore, light as the trigger can be completely removed quickly on-demand.[12] Other than the rapidness and cleanness, light can even realize a precise regulation at a nanometer size. The reversibility of our vesicles' formation governed by light was studied using DLS and TEM. As shown in Figure 6/7 and Table 2, upon UV irradiation for 30 min, the particles' diameter sizes decrease significantly and particles with irregular shapes were observed. Then, upon visible light irradiation again, the size distribution and vesicular structures can be recovered. The recovered vesicles shown in Figure 6 (C) and (D) show more rigid and shrunk structure compared with the original ones in Figure 1 (A) and (B). This could be ascribed to the water escape from the core during the vesicle-reconstruction procedure. The results show fine reproducibility of the size distribution and morphology investigated by DLS and TEM. It is interesting that in PBS media, some cross-linked vesicles were found upon recovery by visible light (Figure S26).

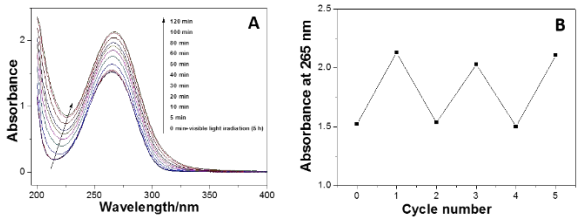

Figure 8. (A) UV/vis spectra of β-CD/**1** in water for increasing durations of UV irradiation (λ = 365 nm) of 0, 5, 10, 20, 30, 40, 50, 60, 80, 100, 120 min (shown from down to top) and the spectrum of the recovered sample upon visible light irradiation (λ = 434 nm) for 5 h; (B) Absorbance changes at 265 nm of β-CD/**1** in water with alternating UV and visible light irradiation.

We studied the UV-induced isomerization of **1** by UV/vis absorption spectroscopy (Figure 8) and ^{1}H NMR (Figure 9, Figure S27). UV/vis spectra of β-CD/**1** after UV irradiation (λ = 365 nm) for different durations at room temperature was undertaken as shown in Figure 8. A caused substantial change in the UV/vis spectra was observed. As the irradiation went on, the absorption peak at 265 nm increased gradually and moved slightly to 267 nm. Meanwhile, the wave trough at 214 nm shifted remarkably to 226 nm. These phenomenon can be ascribed to the isomerization of the *azo* groups from *trans* (π-π*) to *cis* (n-π*) form.[51] The UV-irradiated sample was subjected to visible light irradiation at 434 nm at room temperature for 5 h, and the corresponding spectrum was in good coherence with the 0 min one, which indicates the favorable reverse isomerization.[52]

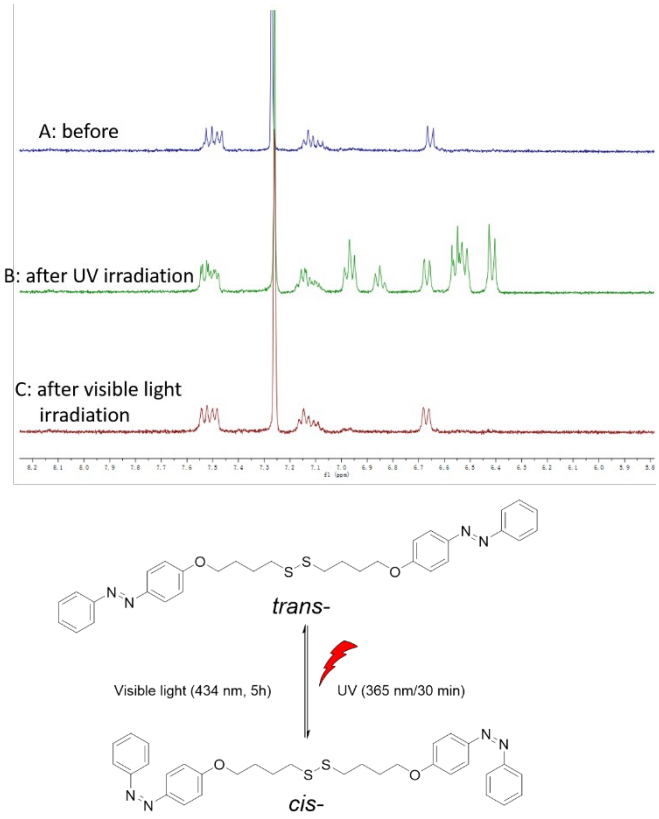

Figure 9. Enlarged ^{1}H NMR spectra (400 MHz in mixed $CD_3OD/CDCl_3$ (2/1 v/v) at 298 K) from the same tube of **1** before (A), after (B) UV irradiation (365 nm, 60 mW·cm^{-2}, 30 min) and (C) visible light irradiation (λ = 434 nm, 20 mW·cm^{-2}, 5 h).

Based on the ^{1}H NMR spectra (Figure 9), approximately 64% of the *trans* isomers switched to *cis* isomers after 365 nm UV irradiation for 30 min (60 mW·cm^{-2}). The new peaks' chemical shifts are in accordance with the previous report.[53] The whole version can be found in Figure S26. It was reported that the *cis* **1** could change back to *trans* isomers by heating or visible light irradiation. The photoresponse indicated in Figure 9 would have to be a sequential two photon process in order to isomerize the two *azo*benzene moieties. Then after visible light irradiation for 5 h, nearly all the *cis* isomers switched back to the *trans* isomers according to the ^{1}H NMR spectra, proving the favorable reversibility of **1**. Quantitive research have been reported that β-CD can include the *trans azo*benzene into its cavity but not the *cis* one.[54] Thus, we have reason to deduce that after UV irradiation, the *cis* **1** could be liberated from the cavity of β-CD, and caged back to the cavity after the visible light irradiation, leading the reversible assembly-disassembly of this superamphiphiles. During the reversible photo-responsive procedure, the steric effects should predominate in the formation of complex with respect to hydrogen bonds.[55] The reversible light-responsive procedure can be repeated at least 5 times.

View Article Online
DOI: 10.1039/C6RA05808F

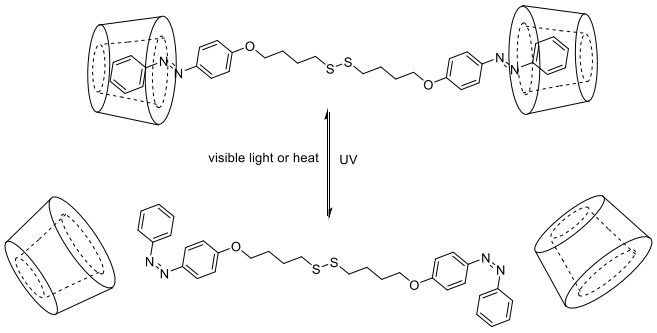

Figure 10. The illustration of the photo-responsive mechanism

The vesicles can undergo disassembly and assembly reversibly by light irradiation because of the photo isomerization of the *azo* group (Figure 10, Figure S20). The light-switchable property can be applied in designing photo-tailored microstructures.

Redox-responsive

The major drawback of light-triggered drug delivery is the low penetration depth (~10 mm) that results from the strong scattering properties of soft tissues. It should be of great advantage if we can combine other endogenous co-activators (for example, highly expressed GSH in tumor cells) into the same system for dual regulation. It is known that DTT is a widely-used reductant to cleave the disulfide bonds.[56] Excess DTT was added to the vesicular solution and it was found that the vesicles disappeared by DLS (Scheme 2 (A)) and TEM (Figure S28). The DTT-treated dispersion (100 mL) was extracted by Et_2O (3 × 100 mL), and compound **3** can be isolated by a flash column chromatography. The structure was confirmed by TLC and MS-ESI results. Hence, we deduce that after the cleavage of the disulfide bond by DTT, compound **3** will be liberated from the dimer. It could be deduced that compound **3** owns too limit hydrophobic volume to play as the hydrophobic tail of the superamphiphiles, which prevents the formation of vesicles. It was reported that the included guest's single alkyl chain should possess at least 6 carbon to play the role of hydrophobic tail of superamphiphile.[57] As shown in Scheme 2 (A), upon DTT treatment, two independent peaks were found in the DLS results both in pure water and PBS 7.40. Based on the molecular-size calculation after energy minimized (Figure S20), the peak around 1 nm could be ascribed directly from β-CD, while the peak around 3 nm from the dissociative β-CD/**3** complex. The peak distribution was further confirmed by comparing with the DLS results of β-CD/**3** in water and β-CD in PBS 7.40 (Figure S29). It is interesting that in pure water, β-CD/**3** complex is still somehow stable, and in PBS 7.40 buffer, the complex tends to be dissociated, which could be due to the stronger electrostatic repulsion in saline media. The second peaks with larger sizes should be resulted from the precipitated compound **3**. GSH, highly expressed in tumor cells, was also tested as the reducing agent and found to have similar effect as DTT.

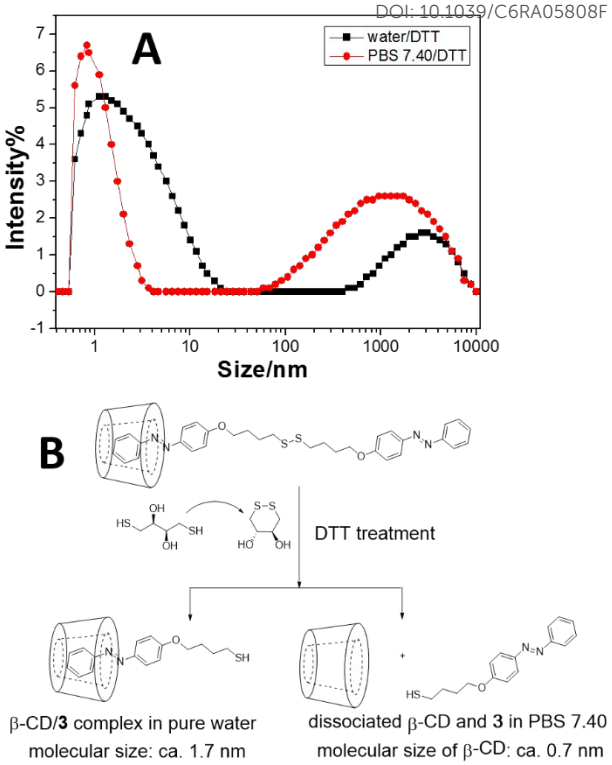

Scheme 2. (A) DLS results of the β-CD/**1** vesicles upon DTT treatment in the aqueous solution at 300 K (black: in pure water; red: in PBS 7.40); (B) the illustration of possible mechanism and molecular sizes after energy minimization.

Drug loading and triggered drug-release

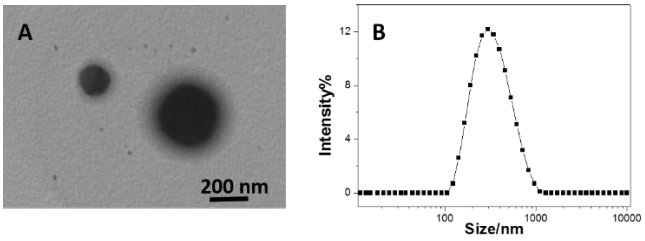

Figure 11. A: TEM micromorphology images (A) and DLS result (B) of MMC-loaded vesicles in water. Phosphotungstic acid was employed as the negative staining agent.

About 40% of drugs are poorly soluble in aqueous solutions and this number is believed to be still increasing as the development of modern high-throughput screening drug-discovery technologies.[58] Increasing the solubility and dissolution rate are key steps in the drug formulation and delivery process.[12] MMC, which finds use as a chemotherapeutic agent by virtue of its antitumour activity,[59] can serve as a model drug with low aqueous solubility.[11] Obvious characteristic $\nu_{c=c}$ peaks (1729, 3267, 3314, 3450 cm^{-1}) of MMC in the FTIR spectrum of MMC-loaded vesicle sample demonstrate successful carrying of MMC to the vesicular system (Figure S30). The solubility of MMC was increased from 0.9 mg/mL[61] to 4.24 mg/mL by the vesicles. Based on the HPLC qualification (Figure S31, S32), the drug loading coefficient and encapsulating rate were calculated as

28.2 wt% and 27.8%, respectively. Upon the drug loading, the β-CD/**1** vesicles' diameters increase slightly observed from TEM and DLS observations (295 nm, Figure 11). This may be due to the insertion of hydrophobic molecules into the bilayers.[60] The spheres with core–shell structures have significant contrast between the centre and the periphery are regarded with a vesicular structure under TEM observation. We also attempted to load pyrene into the vesicles, but only weak peaks of pyrene can be detected from the FTIR spectrum of dried pyrene-loaded vesicle (Figure S34), suggesting a lower loading rate. This could be ascribed to the poor hydrogen bonds formed between pyrene and the building blocks.

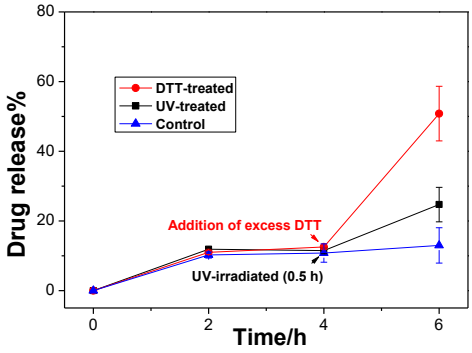

Figure 12. *In vitro* release profiles of MMC-loaded vesicles at 300 K. Blue: no trigger; black: UV irradiated; red: excess DTT added. Values are represented as means ± SD (n = 3).

The drug release upon UV and redox triggers was studied using the classic method of semipermeable membrane. UV light (0.5 h) can trigger 11% more MMC release from the vesicles than control, while the value of DTT trigger can reach 37%. We deduce that after the dissociation of β-CD and **1** triggered by UV, the recovered β-CD cavity can reload MMC.[62] The disulfide bonds are cleaved by DTT, however, the resulting compound **3** can be still caged in β-CD's cavity, excluding partial MMC from the vesicular system. There is competition for the β-CD's complexation among the rest MMC and compound **3**.

Other than the disulfide approach, the design of redox-responsive vesicles can be achieved by employing the functional moieties of ferrocene[63], quinone[64], tetrathiafulvalene[65] or poly (propylene sulphide)[66]. However, there are few reports on redox and light responsive drug carriers.[63] It was known that the disulfide bonds can also be cleaved by highly expressed intracellular GSH in tumor cells.[67] Considering the limit penetrating ability of UV light for the responsiveness, the vesicular systems could be explored in delivering drugs to the surficial targets like mammary and melanoma tumors.[68] Vesicles that can be responsive to near infrared (NIR) light[69] is under development for more applications. It can be concluded that the vesicles are photo-reversible and can be thoroughly destructible by reductants. This could be used in the morphology control during the blood circulation by light to adjust the drug loading rate and a total burst release at the aimed tissue to reach a high drug level.

Conclusions

In this work, we demonstrate a new type of "Bola-type" superamphiphiles with photo and redox-responsive properties. An *azo*benzene dimer linked by disulfide bond was synthesized and can be included by β-CD from both ends to construct a Bola-type superamphiphile in aqueous solution. The superamphiphiles can further self-assemble into dynamic vesicular structure, which is characterized by TEM, *cryo*-TEM and DLS. The formation mechanism of the vesicular structure was suggested based on the results of XRD, FTIR, ^{1}H NMR, NMR-NOESY and UV-vis results. The vesicles will be disrupted upon treatment by UV irradiation and can be recovered by visible light irradiation. Reducing agents like DTT and GSH can cause dispersion of the vesicle clusters *via* breaking the disulfide bond. We attempted to employ the vesicles to load antitumor drug MMC. Upon stimuli, the drug release can be significantly promoted. We believe the study can enrich the topology structure of superamphiphiles and cast a new light on the facile design of noninvasive stimuli-responsive materials.

Acknowledgements

This work was supported by the Scientific Research Foundation of Fudan University for Talent Introduction (JJF301103), National Science Fund for Distinguished Young Scholars (81425023), National Natural Science Foundation of China (81172993) and Fudan's Undergraduate Research Opportunities Program (FDUROP, SSH6285006/004/021). The authors declare no competing financial interest. The authors appreciate a lot for Mr. Pengyao Xing from Shandong University for the assistance on the careful TEM characterization. Supporting information is available online from the author.

Notes and references

1 X. Zhang and C. Wang, Supramolecular amphiphiles, *Chem. Soc. Rev.*, 2011, **40**, 94–101.
2 Y. Cao, X. Hu, Y. Li, X. Zou, S. Xiong, C. Lin, Y. Shen and L. Wang, Multistimuli-responsive supramolecular vesicles based on water-soluble pillar[6]arene and SAINT complexation for controllable drug release, *J. Am. Chem. Soc.*, 2014, **136**, 10762–10769.
3 P. Xing, T. Sun and A. Hao, Vesicles from supramolecular amphiphiles, *RSC Adv.*, 2013, **3**, 24776–24793.
4 Y. Liu, C. Yu, H. Jin, B. Jiang, X. Zhu, Y. Zhou, Z. Lu and D. Yan, A Supramolecular Janus hyperbranched polymer and its photoresponsive self-assembly of vesicles with narrow size distribution, *J. Am. Chem. Soc.*, 2013, **135**, 4765–4770.
5 I. Tomatsu, A. Hashidzume and A. Harada, Photoresponsive hydrogel system using molecular recognition of α-cyclodextrin, *Macromolecules*, 2005, **38**, 5223–5227.
6 R. Dong, Y. Zhou, X. Huang, X. Zhu, Y. Lu and J. Shen, Functional supramolecular polymers for biomedical applications, *Adv. Mater.*, 2015, **27**, 498–526.
7 Y. Liu, K. Wang, D. Guo and B. Jiang, Supramolecular assembly of perylene bisimide with β-cyclodextrin grafts as a solid-state fluorescence sensor for vapor detection, *Adv. Funct. Mater.*, 2009, **19**, 2230–2235.
8 R. Eelkema, K. Maeda, B. Odell and H. L. Anderson, Radical cation stabilization in a cucurbituril oligoaniline rotaxane, *J. Am. Chem. Soc.*, 2007, **129**, 12384–12385.
9 T. Aida, E. W. Meijer and S. I. Stupp, Functional supramolecular polymers, *Science*, 2012, **335**, 813–817.
10 A. Tsuda, Y. Nagamine, R. Watanabe, Y. Nagatani, N. Ishii and T. Aida, Spectroscopic visualization of sound-induced liquid

vibrations using a supramolecular nanofiber, *Nat. Chem.*, 2010, **2**, 977–983.
11 T. Sun, A. Morger, B. Castagner and J.-C. Leroux, An oral redox-sensitive self-immolating prodrug strategy, *Chem. Commun.*, 2015, **51**, 5721–5724.
12 S. Mura, J. Nicolas and P. Couvreur, Stimuli-responsive nanocarriers for drug delivery, *Nat. Mater.*, 2013, **12 (11)**, 991–1003.
13 R. Labruère, A. Alouane, T. Le Saux, I. Aujard, P. Pelupessy, A. Gautier, S. Dubruille, F. Schmidt and L. Jullien, "Self-immolative" spacer for uncaging with fluorescence reporting, *Angew. Chem. Int. Ed. Engl.*, 2012, **51 (37)**, 9344–9347.
14 K. Chen, H. Liang, H. Chen, Y. Wang, P. Cheng, H. Liu, Y. Xia and H. Sung, A thermoresponsive bubble-generating liposomal system for triggering localized extracellular drug delivery, *ACS Nano*, 2013, **7 (1)**, 438–446.
15 N. Y. Rapoport, A. M. Kennedy, J. E. Shea, C. L. Scaife and K. H. Nam, Controlled and targeted tumor chemotherapy by ultrasound-activated nanoemulsions/microbubbles, *J. Control. Release*, 2009, **138**, 268–276.
16 J. Ge, E. Neofytou, T. J. Cahill, R. E. Beygui and R. N. Zare, Drug release from electric-field-responsive nanoparticles, *ACS Nano*, 2011, **6 (1)**, 227–233.
17 M. B. Bannwarth, S. W. Kazer, S. Ulrich, G. Glasser, D. Crespy and K. Landfester, Well-defined nanofibers with tunable morphology from spherical colloidal building blocks, *Angew. Chem. Int. Ed. Engl.*, 2013, **52**, 10107–10111.
18 P. K. Kundu, D. Samanta, R. Leizrowice, B. Margulis, H. Zhao, M. Börner, T. Udayabhaskararao, D. Manna and R. Klajn, Light-controlled self-assembly of non-photoresponsive nanoparticles, *Nat. Chem*., 2015, **7 (8)**, 646–652.
19 J. H. Ryu, R. T. Chacko, S. Jiwpanich, S. Bickerton, R. P. Babu and S. Thayumanavan, Self-cross-linked polymer nanogels: a versatile nanoscopic drug delivery platform, *J. Am. Chem. Soc.*, 2010, **132**, 17227–17235.
20 J. H. Schenkel, A. Samanta and B. J. Ravoo, Self-assembly of soft hybrid materials directed by light and a magnetic field, *Adv. Mater.*, 2014, **26**, 1076–1080.
21 Y. Zhang, J. W. Chanb, A. Morettia and K. E. Uhrich, Designing polymers with sugar-based advantages for bioactive delivery applications, *J. Control. Release*, 2015, **219**, 355–368.
22 A. Alsbaiee, B. J. Smith, L. Xiao, Y. Ling, D. E. Helbling and W. R. Dichtel, Rapid removal of organic micropollutants from water by a porous β-cyclodextrin polymer, *Nature*, 2016, **529**, 190–194.
23 T. M. Allen and P. R. Cullis, Drug delivery systems: entering the mainstream, *Science*, 2004, **303**, 1818–1822.
24 S. M. Christensen and D. Stamou, Surface-based lipid vesicle reactor systems: fabrication and applications, *Soft Matter*, 2007, **3**, 828–836.
25 D. E. Discher and A. Eisenberg, Polymer vesicles, *Science*, 2002, **297**, 967–973.
26 N. O. Mahmoodi, A. Ghavidast, S. Mirkhaef and M. A. Zanjanchi, Photochromism of azobenzene-thiol-1, 3-diazabicyclo-[3.1.0]hex-3-ene on silver nanoparticles, *Dyes Pigments*, 2015, **118**, 110–117.
27 J. Zou, F. Tao and M. Jiang, Optical switching of self-assembly and disassembly of noncovalently connected amphiphiles, *Langmuir*, 2007, **23**, 12791–12794.
28 K. Uekama, F. Hirayama and T. Irie, Cyclodextrin drug carrier systems, *Chem. Rev.*, 1998, **98**, 2045–2076.
29 P. S. K. Gehlot, S. Rao, P. Bharmoria, K. Damarla, H. Gupta, M. Drechsler and A. Kumar, Spontaneous formation of multiarchitecture vesicles of [C8mim]Br + [Na]DBS in aqueous medium: synergic interplay of electrostatic, hydrophobic, and π–π stacking interactions, *J. Phys. Chem. B*, 2015, **119** (49), 15300–15309.
30 Q. Zhang, Y. Liao, L. He and W. Bu, Spherical polymer brushes in solvents of variable quality: an experimental insight by TEM imaging, *Langmuir*, 2013, **29 (13)**, 4181–4186.
31 J. R. S. Martin, I. Bihannic, C. Santos, J. P. S. Farinha, B. Demé, F. A. M. Leermakers, J. P. Pinheiro, E. Rotureau and J. F. L. Duval, Structure of multiresponsive brush-decorated nanoparticles: a combined electrokinetic, DLS, and SANS study, *Langmuir*, 2015, **31 (16)**, 4779–4790.
32 Y. Kim and M. Lee, Supramolecular capsules from bilayer membrane scission driven by corannulene, *Chem. Eur. J.*, 2015, **21**, 5736–5740.
33 R. Tamate, T. Ueki, M. Shibayama and R. Yoshida, Self-oscillating vesicles: spontaneous cyclic structural changes of synthetic diblock copolymers, *Angew. Chem. Int. Ed.*, 2014, **53**, 11248–11252.
34 T. Sun, Q. Guo, C. Zhang, J. Hao, P. Xing, J. Su, S. Li, A. Hao and Liu, G. Self-assembled vesicles prepared from amphiphilic cyclodextrins as drug carriers, *Langmuir*, 2012, **28**, 8625–8636.
35 R. Maurice, M. L. Eftink, K. Bystrom, H. D. Perlmutter and D. S. Kristol, Cyclodextrin inclusion complexes: studies of the variation in the size of alicyclic guests, *J. Am. Chem. Soc.*, 1989, **111**, 6765–6772.
36 Q. Zhao, Y. Wang, Y. Yan and J. Huang, Smart nanocarrier: self-assembly of bacteria-like vesicles with photoswitchable cilia, *ACS Nano*, 2014, **8 (11)**, 11341–11349.
37 K. Zhu, C. A. O'Keefe, V. N. Vukotic, R. W. Schurko and S. J. Loeb, A molecular shuttle that operates inside a metal–organic framework, *Nat. Chem.*, 2015, **7**, 514–519.
38 W. Yin and M. Z. Yates, Effect of interfacial free energy on the formation of polymer microcapsules by emulsification/freeze-drying, *Langmuir*, 2008, **24 (3)**, 701–708.
39 P. L. Nostro, I. Santoni, M. Bonini and P. Baglioni, Inclusion compound from a semifluorinated alkane and β-cyclodextrin, *Langmuir*, 2003, **19**, 2313–2317.
40 W. Weng, Z. Li, A. M. Jamieson and S. J. Rowan, Control of gel morphology and properties of a class of metallo-supramolecular polymers by good/poor solvent environments, *Macromolecules*, 2009, **42**, 236–246.
41 G. Li and L. B. McGown, Molecular nanotube aggregates of β- and γ-cyclodextrins linked by diphenylhexatrienes, *Science*, 1994, **264**, 249–251.
42 J. H. Jung, G. John, M. Masuda, K. Yoshida, S. Shinkai and T. Shimizu, Self-assembly of a sugar-based gelator in water: Its remarkable diversity in gelation ability and aggregate structure, *Langmuir*, 2001, **17**, 7229–7232.
43 H. J. Schneider, F. Hacket, V. Rüdiger and H. Ikeda, NMR studies of cyclodextrins and cyclodextrin complexes, *Chem. Rev.*, 1998, **98**, 1755–1785
44 S. Hu, J. Li, J. Xiang, J. Pan, S. Luo and J. Cheng, Asymmetric supramolecular primary amine catalysis in aqueous buffer: connections of selective recognition and asymmetric catalysis, *J. Am. Chem. Soc.*, 2010, **132 (20)**, 7216–7228.
45 D. Bardelang, A. Rockenbauer, H. Karoui, J. P. Finet and P. Tordo, Inclusion complexes of PBN-type nitrone spin traps and their superoxide spin adducts with cyclodextrin derivatives: parallel determination of the association constants by NMR titrations and 2D-EPR simulations, *J. Phys. Chem. B*, 2005, **109**, 10521–10530.
46 P. MacCarthy, Simplified experimental route for obtaining Job's curves, *Anal. Chem.*, 1978, **50**, 2165.
47 W. An, H. Zhang, L. Sun, A. Hao, J. Hao and F. Xin, Reversible vesicles based on one and two head supramolecular cyclodextrin amphiphile induced by methanol, *Carbohyd. Res.*, 2010, **345**, 914–921.
48 G. M. Escandar, Spectrofluorimetric determination of piroxicam in the presence and absence of β-cyclodextrin, *Analyst*, 1999, **124**, 587–591.

49 G. Crini, Review: a history of cyclodextrins, *Chem. Rev.*, 2014, **114**, 10940−10975.
50 M. V. Rekharsky and Y. Inoue, Complexation thermodynamics of cyclodextrins, *Chem. Rev.*, 1998, **98**, 1875−1917.
51 A. Prestel and H. M. Möller, Spatio-temporal control of cellular uptake achieved by photoswitchable cell-penetrating peptides, *Chem. Commun.*, 2016, **52**, 701−704.
52 T. Liu, C. Bao, H. Wang, Y. Lin, H. Jia and L. Zhu, Light-controlled ion channels formed by amphiphilic small molecules regulate ion conduction via cis-trans photoisomerization, *Chem. Commun.*, 2013, **49**, 10311−10313.
53 D. Wang, M. Wagner, H.-J. Butt and S. Wu, Supramolecular hydrogels constructed by red-light-responsive host–guest interactions for photo-controlled protein release in deep tissue, *Soft Matter*, 2015, **11**, 7656−7662.
54 Y. P. Wang, N. Ma, Z. Q. Wang and X. Zhang, Photo-controlled reversible supramolecular assembly of an azobenzene-containing surfactant with α-cyclodextrin, *Angew. Chem. Int. Ed.*, 2007, **49**, 2823−2826.
55 A. Nakamura and Y. Inoue, Electrostatic manipulation of enantiodifferentiating photocyclodimerization of 2-anthracenecarboxylate within γ-cyclodextrin cavity through chemical modification. Inverted product distribution andenhanced enantioselectivity, *J. Am. Chem. Soc.*, 2005, **127**, 5338−5339.
56 W. W. Cleland, Dithiothreitol, a new protective reagent for SH groups, *Biochemistry*, 1964, **3**, 480−482.
57 T. Sun, H. Zhang, H. Yan, J. Li, G. Cheng, A. Hao, H. Qiao and F. Xin, Sensitive fluorescent vesicles based on the supramolecular inclusion of β-cyclodextrins with N-alkylamino-1-anthraquinone, *Supramol. Chem.*, 2011, **23 (5)**, 351−364.
58 J. Rautio, H. Kumpulainen, T. Heimbach, R. Oliyai, D. Oh, T. Jarvinen and J. Savolainen, Prodrugs: design and clinical applications, *Nat. Rev. Drug Discov.*, 2008, **7**, 255−270.
59 J. Renault, M. Baron and P. Mailliet, Heterocyclic quinones 2. Quinoxaline-5,6-(and 5-8)-diones - Potential antitumoral agents, *Eur. J. Med. Chem.*, 1981, **16 (6)**, 545−550.
60 J. X. Zhang, X. D. Li, M. Q. Yan, L. Y. Qiu, Y. Jin and K. J. Zhu, Hydrogen bonding-induced transformation of network aggregates into vesicles-A potential method for the preparation of composite vesicles, *Macromol. Rapid Commun.*, 2007, **28 (6)**, 710−717.
61 T. Kakutani, R. Atsumi, E. Sumimoto and M. Hashida, Deconvolution analysis of the regeneration process of mitomycin C from prodrug in a muscle perfusion system based on statistical moment theory, *Chem.Pharm. Bull. (Tokyo)*, 1987, **35**, 4907−4914.
62 O. Bekers, J. H. Beijnen, E. H. Groot Bramel, M. Otagiri, A. Bult and W. J. M. Underberg, Stabilization of mitomycins on complexation with cyclodextrins in aqueous acidic media, *Inter. J. Pharmaceut.*, 1989, **52 (3)**, 239−248.
63 A. Samanta and B. J. Ravoo, Metal Ion, light, and redox responsive interaction of vesicles by a supramolecular switch, *Chem. Eur. J.*, **2014**, *20*, 4966−4973.
64 W. Ong, Y. Yang, A. C. Cruciano, and R. L. McCarley, Redox-triggered contents release from liposomes, *J. Am. Chem. Soc.*, **2008**, *130*, 14739−14744.
65 K. D. Zhang, T. Y. Zhou, X. Zhao, X. K. Jiang, and Z. T. Li, Redox-responsive reverse vesicles self-assembled by pseudo[2]rotaxanes for tunable dye release, *Langmuir*, **2012**, *28*, 14839−14844.
66 A. Napoli, M. Valentini, N. Tirelli, M. Müller and J. A. Hubbell, Oxidation-responsive polymeric vesicles, *Nat. Mater.*, **2004**, *3*, 183−189.
67 Y. Zhang, Q. Yin, J. Yen, J. Li, H. Ying, H. Wang and Y. Hua, Chaney, E. J.; Boppart, S. A.; Cheng, J. Non-invasive, real-time reporting drug release *in vitro* and *in vivo*. *Chem. Commun.*, 2015, **51**, 6948−6951.
View Article Online
DOI: 10.1039/C6RA05808F
68 S. Monti and I. Manet, Supramolecular photochemistry of drugs in biomolecular environments, *Chem. Soc. Rev.*, 2014, **43**, 4051−4067.
69 B. Yan, J.-C. Boyer, N. R. Branda and Y. Zhao Near-infrared light-triggered dissociation of block copolymer micelles using upconverting nanoparticles, *J. Am. Chem. Soc.*, 2011, **133**, 19714−19717.

View Article Online
DOI: 10.1039/C6RA05808F

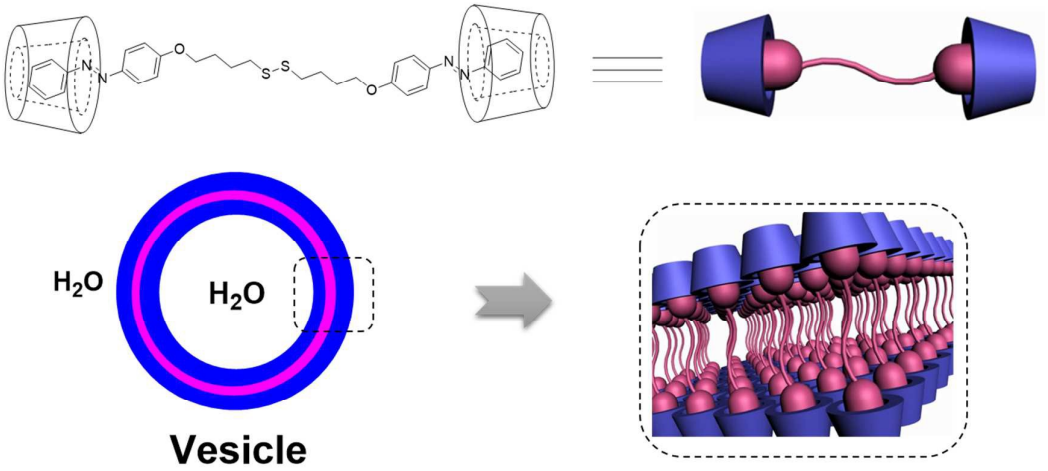

Photo and redox-responsive vesicles assembled from “Bola-type” superamphiphiles were developed.